

Mechanisms Involved in Kjeldahl Microwave Digestion of Amino Acids

Carolle L. Suard,[†] Rose-Marie Mourel,[†] Dominique Didenot,[‡] and Max H. Feinberg^{*,†}

Laboratoire de Chimie analytique, Institut National de la Recherche Agronomique, 16 rue Claude Bernard, 75231 Paris Cedex 05, France, and Centre de Recherche de Décines, Rhône Poulenc Industrialisation, B.P. 166, 69151 Décines Charpieu Cedex, France

The high flexibility of open vessel microwave digestion gives one the opportunity to follow the stepwise degradation of amino acids in the presence of H₂SO₄ and H₂O₂. Thus, it is possible to demonstrate, for several amino acids, that only a stoichiometric fraction of nitrogen (called the *easy* fraction) is digested when sulfuric acid is used alone. The other *difficult* fraction is totally dissolved when hydrogen peroxide is added. These first results confirm the use of two-step digestion procedures as described in earlier works. The first step consists in charring the matrix, the second in oxidizing. When considering amino acids that contain an aromatic ring, such as tryptophan and histidine, it is possible to use UV spectrometry to give indications on the intermediate products formed during the charring step. It was assumed that, at least, three compounds are formed and their probable structure, for tryptophan, can be confirmed by ¹H and ¹³C NMR. It is then possible to propose a general digestion mechanism involving sulfonation followed by the opening of the aromatic ring.

Keywords: *Kjeldahl nitrogen; microwave digestion; tryptophan; hydrogen peroxide*

1. INTRODUCTION

It is now clearly established that microwave sample digestion technology has completely modified sample preparation. The most remarkable feature consists in a significant reduction of the digestion time. When compared to traditional digestion methods, this technology also exhibits very good repeatability. In the validation of Kjeldahl nitrogen digestion procedures in food samples, it was demonstrated that a relative standard deviation of repeatability of about 1% can easily be achieved. The very accurate definition of experimental conditions is also profitable to the reproducibility. It facilitates the transfer of microwave procedures from one laboratory to another (Suard et al., 1993). While traditional digestion procedures were usually described as recipes, it is possible to strictly define microwave digestion procedures in terms of reagent volumes, time, and amounts of transferred energy. For instance, we were able to adequately model energy transfers occurring between the different compartments of a reaction vessel—i.e. reaction medium, glassware, oven cavity, and environment—in a focused microwave field and compare the efficiency of a microwave heating system with that of a classical electrical heating plate device (Suard et al., 1996).

Some years ago, the concept of encapsulation was proposed to illustrate this new opportunity to describe a digestion procedure as a global physical chemistry process. An encapsulated digestion technique for a matrix should be described in terms of energy and chemical reactions so that it can be transferred to any digestion device. This new approach is now made possible thanks to the great flexibility of microwave

digestion systems. However, the little knowledge that we have on the chemical reactions involved in the digestion restricts the ability to correctly predict the behavior of any matrix type.

Therefore, an efficient technique for optimizing digestion procedures still consists in building empirical models based on the response surface methodology (Gonon and Mermet, 1992). Using an open vessel focused microwave digester for the determination of Kjeldahl nitrogen in foods, we were able to describe a general model for the digestion procedure (Feinberg et al., 1993). It is a two-stage process, involving a charring step and an oxidation step as illustrated in Figure 1. The first step reagent is a single volume of sulfuric acid V_{sul} and the second is a volume of hydrogen peroxide V_{oxi} . The procedure can then be described as a time–power diagram with several reagent additions.

It is necessary to classify foods, according to their composition (rich in proteins, rich in carbohydrates, rich in fat, and composite), to optimize the procedure and adapt it to the sample matrix. It is then interesting to use a factorial experimental design involving (i) the power at the end of the charring step P_{char} , (ii) the length of the charring step T_{char} , (iii) the power at the end of the oxidation step P_{oxi} , (iv) the length of the oxidation step T_{oxi} , and (v) the number of additions of the same hydrogen peroxide volume.

Such a procedure is easily transferable from one laboratory to another or from one digester to another, so that a very good reproducibility can be achieved without any special effort.

These results show that if we want to be able to propose more precise guidelines for building a procedure, it is necessary to better understand the chemical reactions involved in the degradation of organic matter. Thus, the goal of this study was to outline the main chemical mechanisms occurring during the nitrogen digestion process. This element was selected because it can be easily determined, even in partially digested samples. We focused the study on the degradation of

* Author to whom correspondence should be addressed (telephone + 33 1 44 08 16 45; fax + 33 1 44 08 16 60; e-mail ciqual@inapg.inra.fr).

[†] Institut National de la Recherche Agronomique.

[‡] Rhône Poulenc Industrialisation.

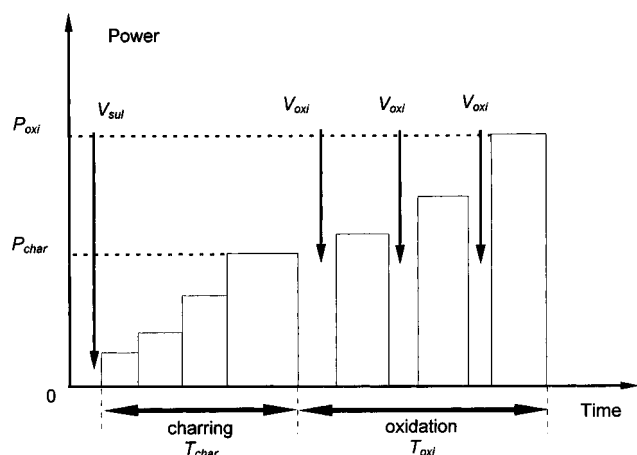


Figure 1. Standard description of a nitrogen digestion procedure.

pure amino acids, as it is easy to compute the global reaction balance by determining the nitrogen recovery yield from the expected nitrogen contents of the molecule.

In the case of Kjeldahl nitrogen, previous papers suggested several mechanisms such as cyclization or dimerization (Bradstreet, 1965), but no recent publications confirm or contradict these hypotheses (Krushavska et al., 1992, 1993). The basic idea was that the very good reproducibility of the process is achieved due to constant chemical reactions.

2. MATERIALS AND METHODS

All experiments were performed on a focused microwave digester Maxidigest MX350 (Prolabo, France). For the determination of Kjeldahl nitrogen, a Kjeltac 1026 (Perstorp) distillation apparatus was used. Five amino acids were selected according to the number of nitrogen atoms in the molecule, the nature of the chemical bond, and their presumed difficulty to be digested. Valine, lysine, and arginine contain an aliphatic chain and, respectively, one, two, and four nitrogen atoms. Tryptophan contains two nitrogen atoms, one of which is included in an imidazole ring. Histidine has three nitrogen atoms, two of which are in a pyrimidine ring. As we were not able to purchase reference molecules with certified composition, theoretical nitrogen content was used to compute recovery yields. All amino acids were obtained from Merck with a concentration "above 99%". Other reagents were purchased at Prolabo: sulfuric acid (95%), hydrogen peroxide (30%), indole, and phenylamine.

For each amino acid an optimized digestion procedure was defined, so that a maximum recovery yield above 99% could be achieved for an aliquot of 0.1 g in the presence of 20 mL of H₂SO₄. Finally, two different procedures were used.

Procedure A (valine and lysine): $P_{\text{char}} = 50\%$, $T_{\text{char}} = 5$ min (one step); $P_{\text{oxi}} = 90\%$, $T_{\text{oxi}} = 10$ min (two steps); and one addition of hydrogen peroxide (total time = 15 min).

Procedure B (arginine, tryptophan, and histidine): $P_{\text{char}} = 50\%$, $T_{\text{char}} = 8$ min (one step); $P_{\text{oxi}} = 90\%$, $T_{\text{oxi}} = 26$ min (four steps); and three additions of hydrogen peroxide (total time = 34 min).

Each hydrogen peroxide addition consisted in 5 mL poured over 2 min. For security reasons, power was set to zero during 1 min after the addition was started. As illustrated in Figure 1, total digestion time includes these periods when the power was set to zero.

Experiments consisted in interrupting the digestion procedure every minute for procedure A and every 2 min for procedure B. As all digest was sampled at each collection time, this means that, respectively, 15 and 17 digests were collected for each procedure. Successive digests were registered as t_0 ,

Table 1. Recovery Yields (Percent) at the End of the Charring and Oxidation Steps

| amino acid | charring step Y_{char} | oxidation step Y_{oxi} | $Y_{\text{char}}/Y_{\text{oxi}}$ |
|------------|---------------------------------|---------------------------------|----------------------------------|
| valine | 98.90 | 98.90 | 1.00 |
| lysine | 72.30 | 98.83 | 0.73 |
| arginine | 69.00 | 97.70 | 0.71 |
| tryptophan | 51.75 | 98.10 | 0.53 |
| histidine | 39.30 | 99.31 | 0.40 |

t_2 , t_4 , up to t_{34} according to their sampling time; t_0 digest consisted only in mixing reagents without any heating.

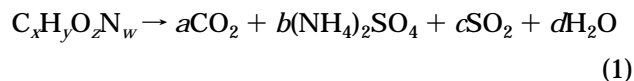
UV spectra were recorded on a Shimadzu spectrophotometer. Before measuring, digests were diluted with water to a final concentration of 4.0×10^{-4} M, so that absorbance remains in the linear response zone of the spectrophotometer. When buffering was necessary, it was achieved with a few milliliters of NaOH. For tryptophan, more descriptive spectra were recorded under acidic conditions, while basic conditions were used for histidine.

NMR spectra were achieved on a Jeol-GLX 400 Hz spectrometer for tryptophan digests. In relation to the very harsh analytical conditions encountered in a digest, three types of spectra were recorded: the first for ¹H after the pH was adjusted to 1 with NaOH, the second for ¹H at pH 7, and the last for ¹³C at pH 7. Deuterated water was used as solvent, and initial tryptophan concentrations were, respectively, 7.4×10^{-2} M (15 g L⁻¹) for ¹H spectra at pH 1, 2.5×10^{-2} M (5 g L⁻¹) for ¹H spectra at pH 7, and 1.2×10^{-1} M (25 g L⁻¹) for ¹³C spectra at pH 7. The reference spectrum for peak identification was achieved on a pure tryptophan solution at pH 1. To improve peak resolution and filter the amine group region that was concealed by a strong H₃O⁺/H₂O signal, a classical signal filtering technique, based on the homogated sequence (or HMG) of the major solvent peak signal, was applied. For some digests, pure tryptophan was also added to confirm the presence of new products. Under these conditions, it was possible to successfully observe the ammonium ion generation from a triplet, at about 52 Hz, formed by coupling of nitrogen and hydrogen as $J(^{14}\text{N}-^1\text{H})$ (Sanders and Hunter, 1988). GC/MS was unsuccessfully applied for identifying digestion products; an adequate extraction procedure could not be achieved.

3. RESULTS

3.1. Evidence for a Two-Stage Digestion Process.

The interesting role of hydrogen peroxide for digesting protein is now well established and commonly used for Kjeldahl routine analysis (Hach et al., 1987). Assumed global reaction appraisal is as follows:



Carbon and hydrogen atoms are turned into CO₂ and H₂O, and nitrogen atoms into quaternary ammonium. Oxidation is partly achieved with concentrated sulfuric acid and completed in the presence of H₂O₂, which forms with H₂SO₄ a peroxymonosulfuric acid (H₂SO₅). As it was observed that the addition of H₂O₂ dramatically influenced the reaction rate, we decided to measure the evolution of the nitrogen recovery yield for the five selected amino acids as a function of time, with or without an addition of H₂O₂. Each digestion sequence was replicated three times.

Table 1 summarizes the recovery yields recorded at the end of the charring step (Y_{char}) and at the end of the oxidation step (Y_{oxi}). The excellent precision of measurements is indicated by the very low relative standard deviation of Y_{oxi} : it was below 0.5% when recovery yield was about 95%. Highest recovery yields never reached 100%, as standard purity was always

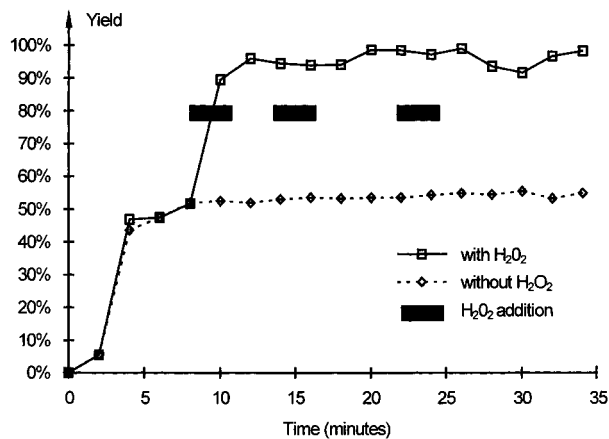


Figure 2. Tryptophan recovery as a function of time.

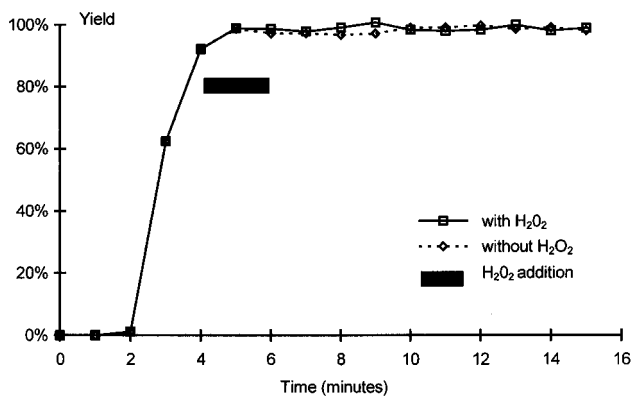


Figure 3. Valine recovery as a function of time.

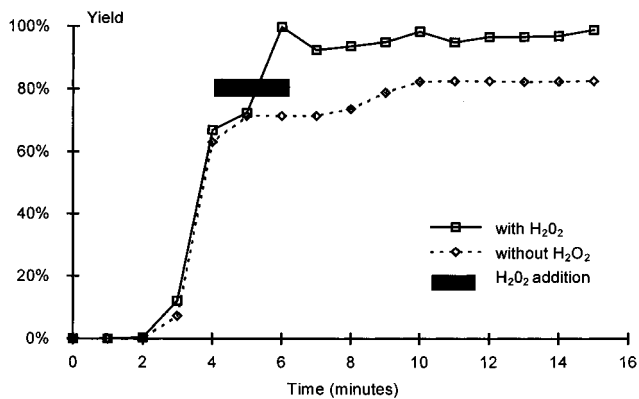


Figure 4. Lysine recovery as a function of time.

claimed as below 99%. Sometimes even lower recovery yields of about 98% were obtained. So, in order to test if any nitrogen was evaporated during digestion, the vapors formed were collected and condensed and their NH_4^+ contents measured. However, no detectable amount of nitrogen was present in this distillate.

Recovery yield profiles for tryptophan, valine, lysine, and histidine are illustrated in Figures 2–5. All data are presented in a similar way: recovery from total digestion in the presence of H_2O_2 as a open square, recovery from partial digestion without H_2O_2 as a diamond, and H_2O_2 addition as a solid square. Temperature was recorded during experiments, and a typical temperature diagram is reported in Figure 2. Light decline after each hydrogen peroxide addition corresponds to the modification of power that was set to zero.

The arginine profile was comparable to that of lysine and is not illustrated. For valine, both curves (with and

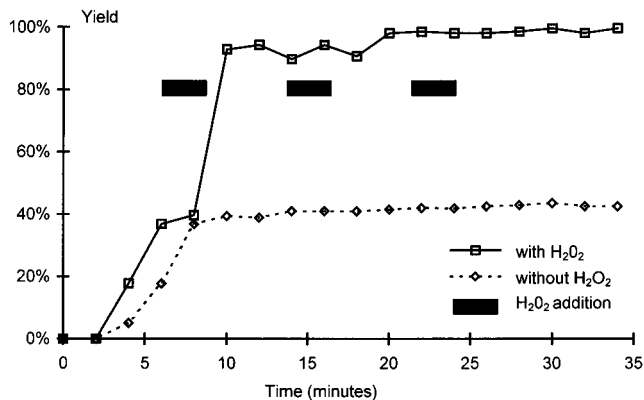
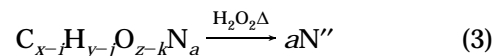
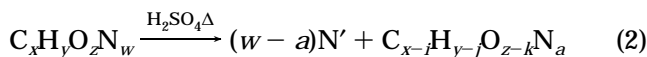


Figure 5. Histidine recovery as a function of time.

without H_2O_2) are identical: maximum recovery yield is reached after 5 min and peroxide was useless. For other amino acids, the two profiles do not overlap. These results clearly demonstrate that the model of charring and oxidation steps, illustrated in Figure 1, actually corresponds to a chemical transformation.

For most molecules, only a proportion of total nitrogen is made soluble before H_2O_2 is added. This proportion is estimated by the $Y_{\text{char}}/Y_{\text{oxi}}$ ratio in Table 1, which approximately corresponds to the stoichiometric proportion of one nitrogen atom. For instance, in the case of tryptophan, the theoretical proportion is 0.50, while the observed ratio is 0.53. The same data for histidine are, respectively, 0.33 and 0.40. It was supposed that amino acid molecules contain *easy* nitrogen atoms, noted N' , and *difficult* atoms, N'' . Thus, a new set of simplified equations can be used to explain the stoichiometric liberation of nitrogen atoms.



In the case of lysine, this hypothesis is not adequate and the formation of dimers or cyclic compounds, such as diketopiperazine, can explain the observed discrepancies. The assumption that the nitrogen that is set free in the first step belongs to the α -amino function was based on the fact that it is possible to obtain a 100% recovery yield from phenylamine by simply applying digestion procedure A. It was decided to focus the rest of the study on aromatic amino acids, because it is possible to obtain degradation products containing rings which can be easily followed by classical spectrometric techniques, such as UV or NMR.

3.2. Degradation Products of Aromatic Amino Acids.

3.2.1. Tryptophan. The first description procedure consisted in recording UV spectra for tryptophan digests at different time intervals in a scanning range of 200 at 400 nm. As illustrated in Figure 6, the UV spectrum for digest t_0 presents a single band I (280 nm). According to the literature, pure tryptophan spectrum in water exhibits an absorption band at 280 nm ($\epsilon = 5660$) which can be related to the indole ring and partly to the carboxylic group. Despite the very strenuous conditions of the digest, it can be assumed that the same chromophores are also absorbing. This spectrum corresponds to a first compound that will be called A_1 , obtained when pure tryptophan and sulfuric acid are mixed. Its structure must be close to that of tryptophan and could be determined by NMR spectroscopy as

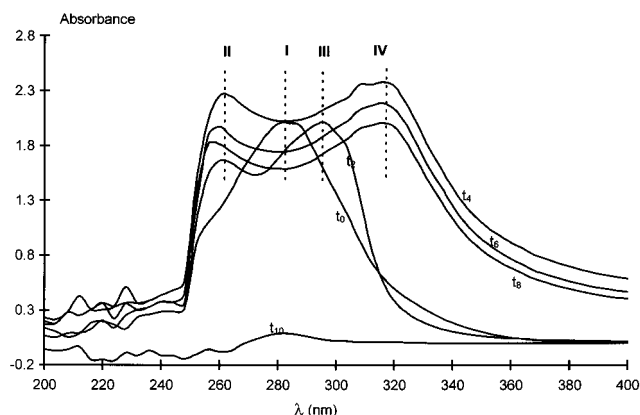


Figure 6. Tryptophan spectra as a function of time (pH 1).

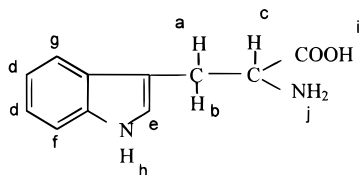


Figure 7. Labeling of tryptophan protons for ^1H NMR.

described further. In digest t_2 , two new bands II (260 nm) and III (296 nm) appeared. While it was observed that the pure indole spectrum at pH 1 presented a maximum absorption band very close to band III, the formed product \mathbf{B}_t was assumed to contain this ring.

The major modification within spectra can be observed after 3 min in digest t_4 . A compound appeared presenting two absorption bands II (260 nm) and IV (318 nm). For digests t_4 – t_8 , bands II and IV were constantly visible but their intensities were decreasing with the time. Thus, it was assumed that only one new compound called \mathbf{C}_t was forming and slowly disappearing. At 10 min after the addition of H_2O_2 , no more absorption band was visible and spectra were completely flat.

Using a classical technique, differential spectra were computed by subtracting the t_0 spectrum corresponding to \mathbf{A}_t from other spectra. Observed negative absorbance values at about 290 nm can be explained by the presence of an indole-containing degradation product present from the first minutes of the digestion that has been called \mathbf{B}_t . The subsequent disappearance of band III indicates that the indole ring is then strongly altered after 3 min. Negative absorbance values can be totally avoided for differential spectra when 80% of the t_0 spectrum is subtracted instead of 100%, indicating that 20% of \mathbf{B}_t is already present in the t_2 digest.

A complementary study of intermediate compounds present in tryptophan digests was realized by ^1H NMR spectrometry after protons were designated according to Figure 7. Tryptophan spectra were completed at pH 1 and 7 on digest.

Table 2 summarizes all observable proton peaks. Results are given for each category of protons and for each pH value used to achieve the NMR spectra. They are expressed as chemical shifts in parts per million, but peak intensity is not reported. The reference spectra were obtained with pure tryptophan solutions buffered at, respectively, pH 1 and 7. In the first five columns, protons that can be related to tryptophan are reported. Unknown product peaks are denoted AR_1 and AR_2 when corresponding to new aromatic compounds and AM_1 for a new amine group.

At pH 1, all reference protons are well identified, except for the carboxylic group proton, which is combined with the $\text{H}_2\text{O}/\text{H}_3\text{O}^+$. By adding pure tryptophan to the t_0 digest, it was possible to establish that a new unknown aromatic compound was present and that the (h) and (j) proton environment was modified: this was called \mathbf{A}_t . Starting from digest t_4 , all protons that could be directly related to tryptophan have disappeared, while NH_4^+ and unknown aromatic and amine protons can easily be identified. As observed with the 7.2 ppm triplet, NH_4^+ is forming after 2 min and signal intensity increases with time. While new AR_1 aromatic protons remain visible from t_0 to t_8 with growing intensity, aliphatic protons completely disappear and the AM_1 proton, between 10.0 and 11.0 ppm, is visible up to digest t_2 .

At pH 7, the comparison between the digest t_0 and the reference spectrum confirmed the early transformation of the tryptophan in \mathbf{A}_t . Aliphatic tryptophan protons were no longer detectable after 4 min. By adding pure tryptophan to digest t_2 , it was observable that the digest peaks were different from the tryptophan peaks. It was confirmed that the new AM_1 peak did not correspond to tryptophan amine protons and that a new product was formed. In the meantime, new aromatic peaks appeared and remained up to digest t_8 , producing specific shifts around 7.6–8.5 and 8.0–9.4 ppm. After H_2O_2 was added, a very significant decrease in all peaks was observed, but the peaks at 7.6–8.0 ppm are still measurable; at this stage, little organic matter remains.

These results fully confirm those obtained by UV spectrometry: a degradation product \mathbf{A}_t is formed just after sulfuric acid is added; it is transformed into at least two other products before being totally destroyed after addition of hydrogen peroxide. The nature of the

Table 2. Summary of ^1H NMR Spectra Peaks (Parts per Million) for Tryptophan Digests at pH 1 and 7

| digest | arom (d–g) | aliph (a–c) | amine 1 (h) | amine 2 (j) | arom AR_1 | amine AM_1 | arom AR_2 | NH_4^+ |
|--------|---------------|----------------|----------------|----------------|-----------------------|------------------------|-----------------------|-----------------|
| pH 1 | | | | | | | | |
| ref | 7.0–7.7 | 3.0–4.1 | 10.2 | 8.0 | | | | |
| t_0 | 7.0–7.9 | 3.6–4.0 | | | 8.0–8.5 | 10.8 | | |
| t_2 | | 2.0–3.0 | | | 7.8–8.5 | 10.0–11.0 | | 7.2 |
| t_4 | | <i>a</i> | | | 7.8–9.8 | | | 7.2 |
| t_6 | | | | | 7.8–9.8 | | | 7.2 |
| pH 7 | | | | | | | | |
| ref | 7.0–7.9 | 3.2–3.7 | 10.3 | | | | | |
| t_0 | 7.6–8.5 | 3.4–3.7 | | | 7.6–8.5 | 10.8 | | |
| t_2 | 7.6–8.0 | 3.4–3.7 | | | 7.7–8.5 | 10.8 | | |
| t_4 | 7.6–8.0 | <i>a</i> | | | 7.6–8.5 | | 8.0–9.4 | |
| t_6 | 7.6–8.0 | <i>a</i> | | | 7.6–8.5 | | 8.0–9.4 | |
| t_8 | 7.6–8.0 | | | | 7.6–8.5 | | 8.0–9.4 | |

^a Peak may still be present but below detection limit and concealed by HDO peak.

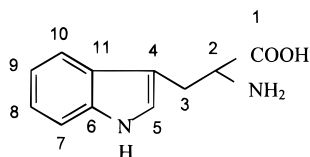


Figure 8. Labeling of tryptophan carbon atoms for ^{13}C NMR.

Table 3. Summary of the Data Obtained from the ^{13}C NMR Spectra at pH 7

| carbon | chemical shifts (ppm) | | carbon | chemical shifts (ppm) | |
|--------|-----------------------|-------|--------|-----------------------|----------|
| | ref | t_0 | | ref | t_0 |
| 1 | 182.0 | 180.5 | 7 | 110.9 | 128.6 |
| 2 | 55.7 | 57.5 | 8 | 120.9 | 127.9 |
| 3 | 29.5 | 30.0 | 9 | 117.9 | <i>a</i> |
| 4 | 109.7 | 111.8 | 10 | 118.3 | <i>a</i> |
| 5 | 126.5 | 134.7 | 11 | 123.6 | |
| 6 | 135.4 | 139.1 | | | |

^a Chemical shift present but not attributable to reference atoms.

first modification was confirmed by ^{13}C NMR spectrometry. The reference consisted of a tryptophan solution in a phosphate buffer at pH 7. It was compared with the t_0 digest spectrum at the same pH. Carbon atoms were labeled according to Figure 8, and results are summarized in Table 3.

The most important feature consists in the disappearance of the 123.6 ppm signal. If it is assumed that corresponding atoms present close shifts, it is possible to allocate all t_0 digest carbon atoms with those of the reference, except for atom 7, which differs by 18 ppm. This result seems to confirm that the indole ring should still be present in compound \mathbf{A}_t but modified. This modification of the molecule likely consists in altering the ring; from its eight atoms, only five are still measurable. This can be explained by an overlapping of signals for two atoms having the same environment. We assumed that atoms 8 and 9 were good candidates for this overlapping and that sulfonation should occur between them. The presence of the 180.5 ppm shift corresponding to the acid group and the 30.0 and 57.5 ppm shifts of the aliphatic chain could indicate that several other compounds, very close to tryptophan, may also exist during the early stages of the digestion.

In conclusion, a five-step process can be reasonably suggested to explain the experimental data observed during tryptophan digestion.

| step | min | products |
|------|------|---|
| 1 | 0 | formation of sulfonated product \mathbf{A}_t |
| 2 | 1–2 | formation of, at least, one stable product \mathbf{B}_t observable by NMR and UV spectrometry |
| 3 | 3–4 | transformation of \mathbf{B}_t into one or more compounds called \mathbf{C}_t |
| 4 | 5–8 | slow degradation of \mathbf{C}_t observable by UV spectrometry |
| 5 | 9–32 | fast and complete degradation of \mathbf{C}_t after H_2O_2 addition |

3.2.2. Histidine. For pure histidine under basic conditions, a maximum UV absorption band is recorded at 211 nm. It can be related to the imidazole ring and the carboxylic group. Figure 9 presents UV spectra for histidine digests from t_0 up to t_{10} . Like tryptophan digests, no more signal is observed after the addition of hydrogen peroxide (t_{10}). For digest t_0 , maximum absorbance was recorded at band I (211 nm). The new compound, called \mathbf{A}_h , that was likely forming when histidine was put in simple contact with pure H_2SO_4 presents a structure close to that of histidine.

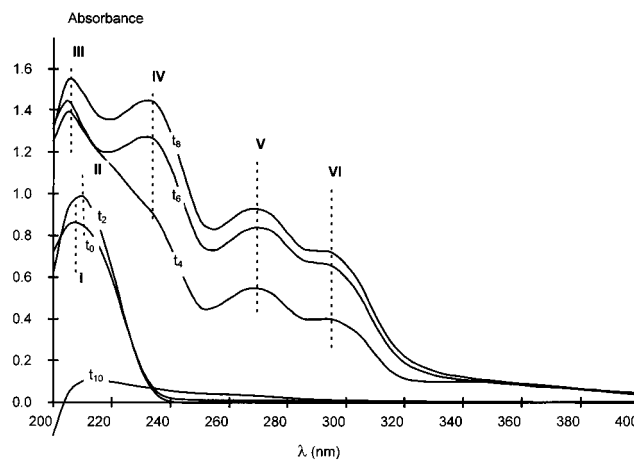


Figure 9. Histidine UV spectra as a function of time (pH 12).

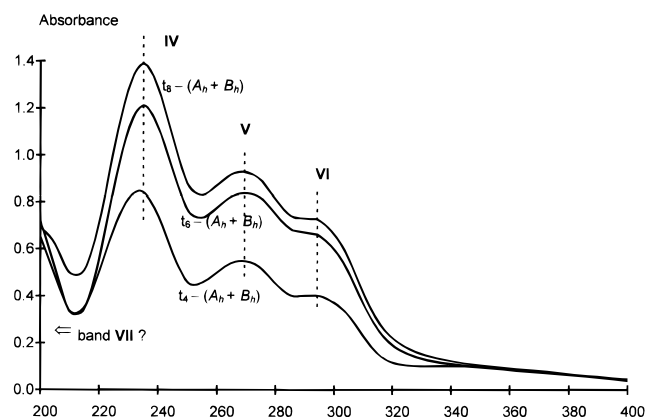


Figure 10. Histidine differential spectra between 4 and 8 min.

The digest t_2 spectrum corresponds to a second compound \mathbf{B}_h with a single absorption band, noted band II (215 nm), which is very close to band I (211 nm). It can be anticipated that the newly formed compound \mathbf{B}_h is likely to contain an imidazole ring. At this moment, the recovery yield is 0% and almost no nitrogen is released (see Figure 5). If it is assumed that the t_0 spectrum corresponds to \mathbf{A}_h , by subtracting it from t_2 , it is possible to confirm that \mathbf{B}_h is formed just after microwave heating is begun. The differential spectrum exhibits a maximum absorption band at 205 nm. Following digests (t_4 – t_8) all contain this same absorption band, identified as band III (205 nm).

Starting from digest t_4 , one or several new compounds are rapidly forming, containing four absorption bands: band III (205 nm), band IV (230 nm), band V (270 nm), and band VI (295 nm). The most striking feature, when these spectra are compared to those of tryptophan digests at the same periods, is that the intensity increases with time instead of decreasing.

To confirm whether one or several products were formed, t_0 and t_2 spectra were subsequently subtracted from the others (Figure 10). For these differential spectra, the intensities of bands IV–VI increase with time (between 4 and 8 min) while their positions are not modified. Thus, it can be assumed that these three bands correspond to three different chromophores which belong to a unique compound that was called \mathbf{C}_h . This new product accumulates and then disappears after 10 min. It must contain at least three chromophores, but the shape of the differential spectrum, below 200 nm, suggests that it may contain a fourth absorption band (band VII) at about 180 or 190 nm.

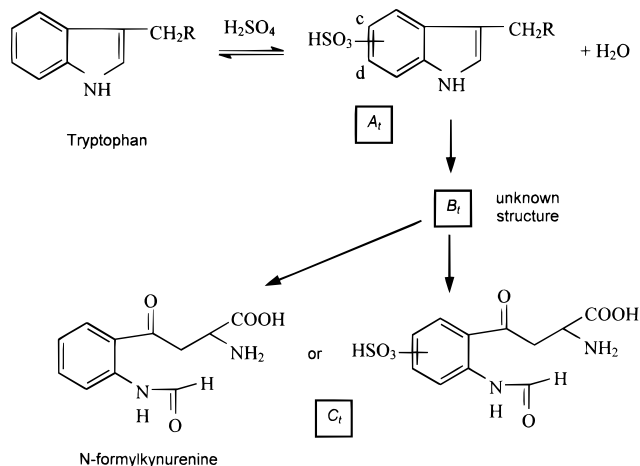


Figure 11. Proposed digestion pathway for tryptophan.

In conclusion, a five-step process can be proposed to explain the reaction mechanisms occurring during histidine digestion.

| step | min | products |
|------|------|---|
| 1 | 0 | formation of product A_h |
| 2 | 1–2 | formation of a stable product B_h observable by UV spectrometry |
| 3 | 3–4 | formation of C_h in the presence of B_h |
| 4 | 5–8 | accumulation of C_h observable by UV spectrometry |
| 5 | 9–32 | fast and complete degradation of B_h and C_h after H ₂ O ₂ addition |

4. DISCUSSION AND CONCLUSION

The hypothesis that some amino acids contain two different kinds of nitrogen atoms, which we called the *easy* and the *difficult* fractions with respect to their transformation into ammonium sulfate in the presence of sulfuric acid, was confirmed by these studies. From the tryptophan ¹H NMR spectra at pH 1, it was quite possible to observe the formation of the ammonium ions from the very beginning of the digestion while aromatic compounds are still present in the reaction medium. The almost immediate breaking of the aliphatic chain, from the second minute of the digestion, and the evidence for an aromatic ring observed by UV spectrometry confirm the second hypothesis that the *easy* fraction is related to the α-amino function.

For tryptophan, the new compound that is formed at the true beginning of the digestion contains an aromatic ring and an amino function, which is shown by a 10.8 ppm chemical shift on ¹H NMR spectra. While signals of aromatic protons (a to d and k) are debled in comparison to those of pure tryptophan and carbon atoms corresponding to positions 5, 8, and 10 are observable as singlets, it can be concluded that there are no associated protons, as for pure tryptophan. This can only be explained by a substitution of the benzene ring between carbons 6 and 7. On the other hand, a double sulfonation is not very probable for steric considerations. Thus, a reversible sulfonation reaction can be proposed (Figure 11).

The compound **A_t** totally disappears between the third and fourth minutes when **B_t** is formed. The most probable hypothesis for **B_t** consists of the opening of the ring. The shift of the signal toward low frequency intensities makes the NMR identification impossible, and **B_t** structure could not be identified. It was assumed that the ring opening occurred by the oxidation of ethylene bound to nitrogen in the α position, forming a ketone and an aldehyde function: this mechanism is

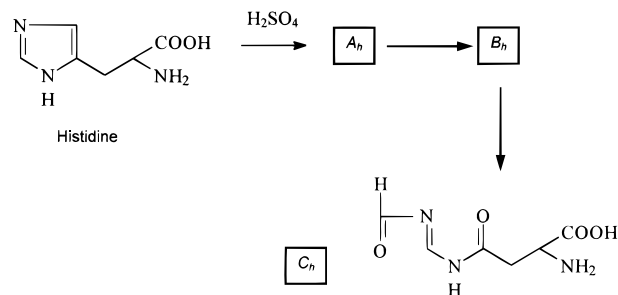


Figure 12. Proposed digestion pathway for histidine.

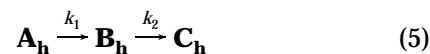
more probable than the opening of the indole ring. The resulting molecules could be the *N*-formylkynurenine or its sulfonated form. According to the literature, *N*-formylkynurenine presents an UV absorption band at 318 nm, at the same wavelength as band IV that was observed in Figure 6 (Walrant et al., 1974; Kell and Steinhart, 1990). These products can still be present in the medium after 10 min, while the nitrogen recovery is only about 90%. However, the great complexity of ¹H NMR spectra may suggest that other compounds may be formed but in lower quantities. These may have a common chromophore with *N*-formylkynurenine, so that they are not detectable by UV spectrometry.

When one is dealing with histidine, while NMR spectra were not available, two reaction mechanisms can be considered:

1. **B_h** and **C_h** form simultaneously



2. **B_h** is an intermediate compound that is transformed into **C_h**



The first hypothesis is more convenient to explain the simultaneous increase and decrease of absorption bands III–VI from the fourth minute. However, the detection of **B_h** in *t*₂ digest and the detection of **C_h** in only *t*₄ digest refute this hypothesis. Moreover, the ratio between absorption band heights should be constant, because molar extinction coefficients are constant. This is not observable. For establishing the second hypothesis, the equilibrium constant *k*₂ must be larger than *k*₁, so that it is possible to explain the accumulation of **C_h** while **B_h** concentration remains constant.

The refutation of the second hypothesis could be based on the fact that **B_h** seems to accumulate between *t*₂ and *t*₈, from observation of band III in Figure 9. However, a closer examination of spectra shows that this apparent increase can be explained by the overlapping of **B_h** and **C_h** spectra. **C_h** exhibits a wide absorption band at 230 nm that is clearly visible when the the differential spectra are considered (see Figure 10). Finally, the second reaction mechanism seems to be the most probable and can be proposed for histidine and tryptophan.

As stated earlier, a fourth absorption band below 200 nm is likely to be present in the **C_h** product and could easily correspond to the conjugation of the carboxylic group an aromatic ring. If this assumption is accepted, it is then possible to propose the following structure for the **C_h** compound (Figure 12) on the basis of the following facts:

- Typical aldehyde and ketone absorption bands are situated between 250 and 300 nm.
- Typical saturated carboxylic acids absorb at around 200 nm.
- Oxime double-bond-conjugated with an aldehyde absorbs at 230 nm (Silverstein et al., 1974).

Unfortunately, the presence of two nitrogen atoms in this molecule did not allow the application of the Woodward–Hoffman model for predicting the UV absorption bands, and a reference spectrum is not available in the literature.

It is interesting to note that both mechanisms proposed for tryptophan and histidine correspond to the same two-step reaction: oxidation of the ethylene double bond followed by opening of the aromatic ring and formation of aldehyde and ketone functions. Therefore, the structure of the C_h compound, formed from histidine, is comparable to that of the C_t (or *N*-formylkynurenine) formed from tryptophan, the additional benzene ring excepted.

In conclusion, it was clearly established that before hydrogen peroxide is added, the percent of soluble nitrogen is almost equal to a stoichiometric proportion, except for aliphatic amino acids. At that moment, the digestion medium still contains several UV-absorbing organic compounds. It was also possible to observe a sequential transformation of tryptophan or histidine byproducts. In spite of the difficult analytical conditions, the use of NMR and UV spectrometry was efficient for discerning clues on their chemical structure.

It is interesting to observe that the formed compounds are very comparable for histidine and tryptophan, and digestion pathways are also comparable. This chemical process is highly repeatable, and the great advantage of microwave technology consists in bringing the required amount of energy in the most convenient way so that the reaction kinetics are optimal. Our proposal for a two-stage digestion procedure involving charring and oxidation is then consistent with the observed chemical behavior of digests.

On the other hand, the considerable modification of remaining organic compounds that can be observed after hydrogen peroxide is added (Figures 3–5) confirms the major importance of this reagent for completely destroying protein macromolecules in biological matrices. This criterion could be used for defining a mineralization termination indicator for any digestion procedure, even

those based on nitric, hydrochloric, or hydrofluoric acids as used for trace element analysis.

LITERATURE CITED

- Bradstreet, R. B. *The Kjeldahl Methods for Organic Nitrogen*; Academic Press: New York, 1965.
- Feinberg, M. H.; Ireland-Ripert, J.; Mourel, R. M. Optimization procedure of open vessel microwave digestion for Kjeldahl nitrogen determination in foods. *Anal. Chim. Acta* **1993**, *272*, 83–90.
- Gonon, L.; Mermet, J. M. Aciers et alliages: savoir choisir un mode de mise en solution rapide pour une analyse élémentaire (Steels and alloys: how to select a fast digestion technique for elementary analysis). *Analisis* **1992**, *20*, M26–M29.
- Hach, C.; Bowden, B.; Kopelove, A.; Brayton S. More powerful peroxyde Kjeldahl digestion method. *J. Assoc. Off. Anal. Chem.* **1987**, *70*, 783–787.
- Kell, G.; Steinhart, H. Oxidation of tryptophan by H_2O_2 in model systems. *J. Food Sci.* **1990**, *55*, 1120–1123.
- Krushevska, A.; Barnes, R. M.; Amarasiriwardena, C. J.; Foner, H.; Martines, L. Comparison of sample decomposition procedures for the determination of zinc in milk by inductively coupled plasma atomic emission spectrometry. *J. Anal. At. Spectrom.* **1992**, *7*, 851–858.
- Krushevska, A.; Barnes, R. M.; Amarasiriwardena, C. J. Decomposition of biological samples for inductive coupled plasma atomic emission spectrometry using open focused microwave digestion system. *Analyst* **1993**, *118*, 1175–1181.
- Sanders, J. K. M.; Hunter, B. K. *Modern NMR Spectroscopy, a Guide for Chemists*; Oxford University Press: Oxford, U.K., 1988.
- Silverstein, R.; Bassler, C.; Morrill, T. *Spectrometric Identification of Organic Compounds*, 3rd ed.; Wiley: New York, 1974.
- Suard, C.; Feinberg, M. H.; Ireland-Ripert, J.; Mourel, R. M. Validation par analyse interlaboratoire de la minéralisation par micro-ondes: application à l'azote Kjeldahl dans les aliments. *Analisis* **1993**, *21*, 287–291.
- Suard, C.; Mourel, R. M.; Cerdan, B.; Bart, G.; Feinberg, M. H. Modelling energy transfer in a focused microwave digester. *Anal. Chim. Acta* **1996**, *318*, 261–273.
- Walrant, P.; Santus, R. *N*-Formyl-kynurenine, a tryptophan photooxidation product, as a photodynamic sensitizer. *Photochem. Photobiol.* **1974**, *19*, 411–417.

Received for review June 12, 1996. Revised manuscript received January 13, 1997. Accepted January 27, 1997.[®]

JF960427I

[®] Abstract published in *Advance ACS Abstracts*, March 1, 1997.